LETTERS

Thermalization and its mechanism for generic isolated quantum systems

Marcos Rigol[1,2], Vanja Dunjko[1,2] & Maxim Olshanii[2]

An understanding of the temporal evolution of isolated many-body quantum systems has long been elusive. Recently, meaningful experimental studies[1,2] of the problem have become possible, stimulating theoretical interest[3–7]. In generic isolated systems, non-equilibrium dynamics is expected[8,9] to result in thermalization: a relaxation to states in which the values of macroscopic quantities are stationary, universal with respect to widely differing initial conditions, and predictable using statistical mechanics. However, it is not obvious what feature of many-body quantum mechanics makes quantum thermalization possible in a sense analogous to that in which dynamical chaos makes classical thermalization possible[10]. For example, dynamical chaos itself cannot occur in an isolated quantum system, in which the time evolution is linear and the spectrum is discrete[11]. Some recent studies[4,5] even suggest that statistical mechanics may give incorrect predictions for the outcomes of relaxation in such systems. Here we demonstrate that a generic isolated quantum many-body system does relax to a state well described by the standard statistical-mechanical prescription. Moreover, we show that time evolution itself plays a merely auxiliary role in relaxation, and that thermalization instead happens at the level of individual eigenstates, as first proposed by Deutsch[12] and Srednicki[13]. A striking consequence of this eigenstate-thermalization scenario, confirmed for our system, is that knowledge of a single many-body eigenstate is sufficient to compute thermal averages—any eigenstate in the microcanonical energy window will do, because they all give the same result.

If we pierce an inflated balloon inside a vacuum chamber, very soon we find that the released air has uniformly filled the enclosure and that the air molecules have attained the Maxwell velocity distribution, the width of which depends only on the total number and energy of the air molecules. Different balloon shapes, placements, or piercing points all lead to the same spatial and velocity distributions. Classical physics explains this 'thermodynamical universality' as follows[10]: almost all particle trajectories quickly begin to look alike, even if their initial points are very different, because nonlinear equations drive them to explore the constant-energy manifold ergodically, covering it uniformly with respect to precisely the microcanonical measure. However, if the system possesses further conserved quantities that are functionally independent of the hamiltonian and each other, then time evolution is confined to a highly restricted hypersurface of the energy manifold. Hence, microcanonical predictions fail and the system does not thermalize.

In contrast, in isolated quantum systems not only is dynamical chaos absent owing to the linearity of time evolution and the discreteness of spectra[11], but also it is not clear under what conditions conserved quantities provide independent constraints on the relaxation dynamics. On the one hand, any operator commuting with a generic, and thus non-degenerate, hamiltonian is functionally dependent on it[14], seemingly implying that conservation of energy is the only independent constraint. On the other hand, even when operators are functionally dependent, their expectation values—considered as functionals of states—generally are not: for example, two states may have the same mean energies but different means of squared energies. For non-degenerate hamiltonians a maximal set of constants of motion with functionally independent expectation values is as large as the dimension of the Hilbert space; examples include the projectors $\hat{P}_\alpha = |\Psi_\alpha\rangle\langle\Psi_\alpha|$ to the energy eigenstates[14] and the integer powers of the hamiltonian[5].

The current numerical and analytic evidence from the study of integrable systems suggests that there exists a minimal set of independent constraints the size of which is much less than the dimension of the Hilbert space but may still be much greater than one. In previous work[3] we showed that an isolated integrable one-dimensional system of lattice hard-core bosons relaxes to an equilibrium characterized not by the usual Gibbs ensemble but by a generalized Gibbs ensemble. Instead of just the energy, the Gibbs exponent contains a linear combination of conserved quantities—the occupation numbers of the eigenstates of the corresponding Jordan–Wigner fermions—the number of which is still only a tiny fraction of the dimension of the Hilbert space. Yet this ensemble works, although the usual one does not, for a wide variety of initial conditions[15] as well as for a fermionic system[16]; it also explains a recent experimental result, the absence of thermalization in the Tonks–Girardeau gas[1]. Thus, although at least some constraints other than the conservation of energy must be kept, it turns out that only a relatively limited number of additional conserved quantities with functionally independent expectation values are needed; adding further ones is redundant.

As it is not clear which sets of conserved quantities—and some are always present—constrain relaxation and which do not, it becomes even more urgent to determine whether or not generic isolated quantum systems relax to the usual thermal state. This question has received increased theoretical attention recently, because of the high levels of isolation[1,2,17] and control[18,19] possible in experiments with ultracold quantum gases. However, despite numerous studies of specific models, there is not yet consensus on how or even whether relaxation to the usual thermal values occurs for non-integrable systems[7]. The conventional wisdom is that it does[8,9], but some recent numerical results indicate otherwise, either under certain conditions[4] or in general[5].

To study relaxation of an isolated quantum system, we considered the time evolution of five hard-core bosons with additional weak nearest-neighbour repulsions, on a 21-site, two-dimensional lattice, initially confined to a portion of the lattice and prepared in their ground state there. Figure 1a shows the exact geometry (see also Supplementary Discussion); the relaxation dynamics begins when the confinement is lifted. Expanding the initial-state wavefunction

[1]Department of Physics and Astronomy, University of Southern California, Los Angeles, California 90089, USA. [2]Department of Physics, University of Massachusetts Boston, Boston, Massachusetts 02125, USA.

in the eigenstate basis of the final hamiltonian $\hat{H}$ as $|\psi(0)\rangle = \sum_\alpha C_\alpha |\Psi_\alpha\rangle$, where $C_\alpha = \langle \Psi_\alpha \mid \psi(0)\rangle$ and the index α ranges over all the basis eigenstates $|\psi_\alpha\rangle$, the many-body wavefunction evolves as $|\psi(t)\rangle = e^{-i\hat{H}t}|\psi(0)\rangle = \sum_\alpha C_\alpha e^{-iE_\alpha t}|\Psi_\alpha\rangle$, where the E_α are the eigenstate energies. Thus, obtaining results that are numerically exact for all times requires the full diagonalization of the 20,349-dimensional hamiltonian. The quantum-mechanical mean of any observable $\hat{A}$ evolves as

$$\langle \hat{A}(t)\rangle \equiv \langle \psi(t)|\hat{A}|\psi(t)\rangle = \sum_{\alpha,\beta} C_\alpha^* C_\beta e^{i(E_\alpha - E_\beta)t} A_{\alpha\beta} \quad (1)$$

where $A_{\alpha\beta} = \langle \Psi_\alpha|\hat{A}|\Psi_\beta\rangle$ and the asterisk denotes complex conjugation. The long-time average of $\langle \hat{A}(t)\rangle$ is then

$$\overline{\langle \hat{A}\rangle} = \sum_\alpha |C_\alpha|^2 A_{\alpha\alpha} \quad (2)$$

We note that if the system relaxes at all, it must be to this value. We find it convenient to think of equation (2) as stating the prediction of a 'diagonal ensemble', $|C_\alpha|^2$ corresponding to the weight that $|\Psi_\alpha\rangle$ has in the ensemble. In fact, this ensemble is precisely the generalized Gibbs ensemble introduced in ref. 3 if as integrals of motion we take all the projection operators $\hat{P}_\alpha = |\Psi_\alpha\rangle\langle\Psi_\alpha|$. Using these as constraints on relaxation dynamics, the theory gives the generalized Gibbs density matrix (or constrained density matrix) $\hat{\rho}_c = \exp\left(-\sum_{\alpha=1}^{D} \lambda_\alpha \hat{P}_\alpha\right)$, where $\lambda_\alpha = -\ln(|C_\alpha|^2)$ and D is the dimension of the Hilbert space. (We note, however, that for the integrable system treated in ref. 3, the generalized Gibbs ensemble was defined using a different, minimal set of independent integrals of motion, the number of which was equal to the number of lattice sites N, which is much less than D.)

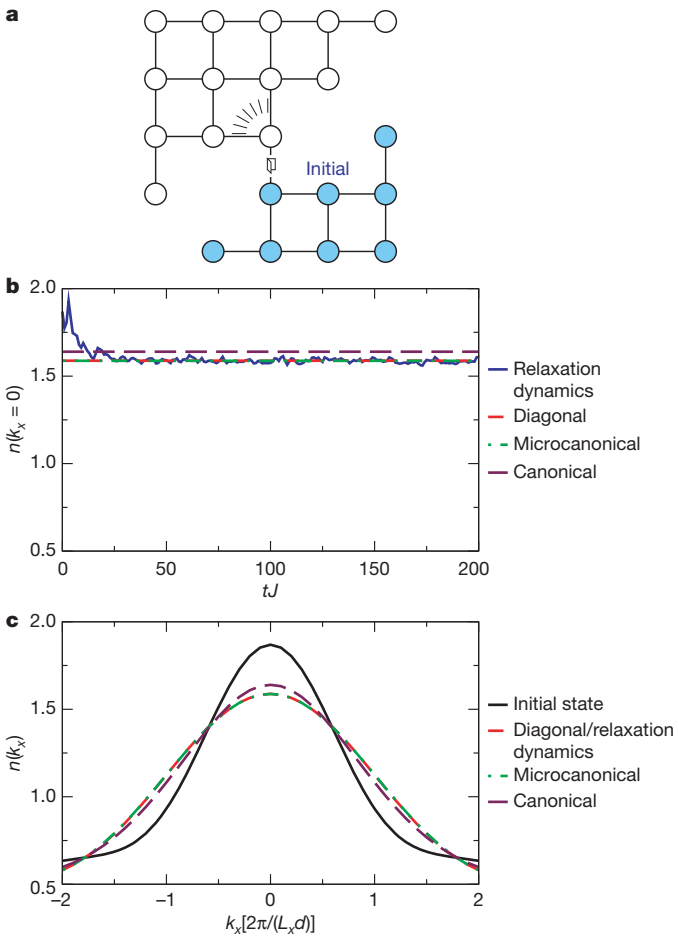

Figure 1 | Relaxation dynamics. a, Two-dimensional lattice on which five hard-core bosons propagate in time. The bosons are initially prepared in the ground state of the sub-lattice in the lower-right corner and released through the link indicated by the drawing of a door. **b**, The corresponding relaxation dynamics of the central component $n(k_x = 0)$ of the marginal momentum distribution, compared with the predictions of the three ensembles, plotted against 'dimensionless time' (in our conventions J, the hopping parameter, has units of inverse time; see Supplementary Information). In the microcanonical case, we averaged over all eigenstates whose energies lie within a narrow window (see Supplementary Discussion) $[E_0 - \Delta E, E_0 + \Delta E]$, where $E_0 \equiv \langle \psi(0)|\hat{H}|\psi(0)\rangle = -5.06J$ and $\Delta E = 0.1J$. The canonical ensemble temperature is $k_B T = 1.87J$, where k_B is the Boltzmann constant, meaning that the ensemble prediction for the energy is E_0. **c**, Full momentum distribution function in the initial state, after relaxation, and in the different ensembles. Here d is the lattice constant and $L_x = 5$ is the lattice width.

The statement that the diagonal and microcanonical ensembles give the same predictions for the relaxed value of $\hat{A}$ reads

$$\sum_\alpha |C_\alpha|^2 A_{\alpha\alpha} = \langle A\rangle_{\text{microcan}}(E_0) \equiv \frac{1}{\mathcal{N}_{E_0,\,\Delta E}} \sum_{\substack{\alpha \\ |E_0 - E_\alpha| < \Delta E}} A_{\alpha\alpha} \quad (3)$$

where E_0 is the mean energy of the initial state, ΔE is the half-width of an appropriately chosen energy window centred at E_0 (see Supplementary Discussion), and the normalization $\mathcal{N}_{E_0,\,\Delta E}$ is the number of energy eigenstates with energies in the window $[E_0 - \Delta E, E_0 + \Delta E]$. Thermodynamical universality is evident in this equality: although the left-hand side depends on the details of the initial conditions through the set of coefficients C_α, the right-hand side depends only on the total energy, which is the same for many different initial conditions. The following three scenarios suggest themselves as possible explanations of this universality (assuming that the initial state is sufficiently narrow in energy, as is normally the case—see Supplementary Discussion).

First, even for eigenstates close in energy, there are large eigenstate-to-eigenstate fluctuations of both the eigenstate expectation values (EEVs) $A_{\alpha\alpha}$ and the eigenstate occupation numbers (EONs) $|C_\alpha|^2$. However, for physically interesting initial conditions, the fluctuations in the two quantities are uncorrelated. A given initial state then performs an unbiased sampling of the distribution of the EEVs $A_{\alpha\alpha}$, resulting in equation (3).

Second, for physically interesting initial conditions, the EONs $|C_\alpha|^2$ almost do not fluctuate at all between eigenstates that are close in energy. Again, equation (3) immediately follows.

Third, the EEVs $A_{\alpha\alpha}$ almost do not fluctuate at all between eigenstates that are close in energy. In this case equation (3) holds without exception for all initial states that are narrow in energy (unlike in the first two scenarios, for which there may be special states that violate equation (3) despite being narrow in energy).

Deutsch and Srednicki independently proposed the third scenario, which, following Srednicki, we call the 'eigenstate thermalization hypothesis (ETH)'[12,13]: the expectation value $\langle \Psi_\alpha|\hat{A}|\Psi_\alpha\rangle$ of a few-body observable $\hat{A}$ in an energy-E_α eigenstate $|\Psi_\alpha\rangle$ of the hamiltonian of a large, interacting many-body system equals the thermal (microcanonical in our case) average $\langle A\rangle_{\text{microcan}}(E_\alpha)$ of $\hat{A}$ at the mean energy E_α

$$\langle \Psi_\alpha|\hat{A}|\Psi_\alpha\rangle = \langle A\rangle_{\text{microcan}}(E_\alpha)$$

The ETH suggests that classical and quantum thermal states have very different natures, as depicted in Fig. 2. Although at present there

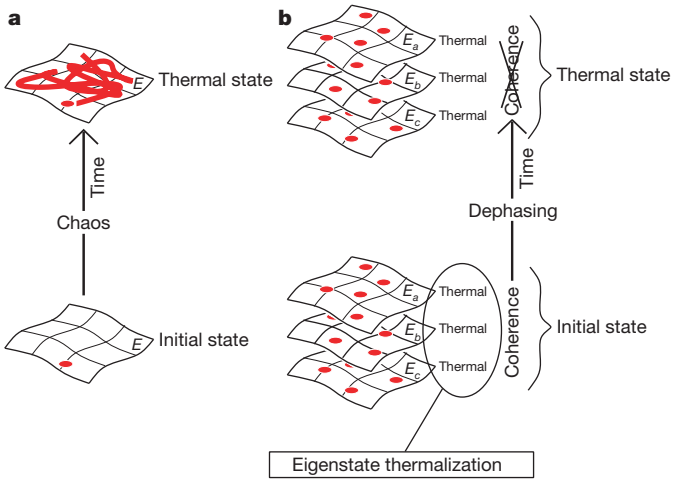

Figure 2 | Thermalization in classical versus quantum mechanics. **a**, In classical mechanics, time evolution constructs the thermal state from an initial state that generally bears no resemblance to the former. **b**, In quantum mechanics, according to the ETH, every eigenstate of the hamiltonian always implicitly contains a thermal state. The coherence between the eigenstates initially hides it, but time dynamics reveals it through dephasing.

are no general theoretical arguments supporting the ETH, some results do exist for restricted classes of systems. For instance, the ETH holds[12] in the case of an integrable hamiltonian weakly perturbed by a single matrix taken from a random gaussian ensemble. Furthermore, nuclear shell model calculations have shown that individual wavefunctions reproduce thermodynamic predictions[20]. There are also rigorous proofs that some quantum systems, whose classical counterparts are chaotic, satisfy the ETH in the semiclassical limit[21–24]. More generally, for low-density billiards in the semiclassical regime, the ETH follows from Berry's conjecture[13,25], which in turn is believed to hold in semiclassical classically chaotic systems[26]. Finally, at the other end of the chaos–integrability spectrum, in systems solvable by Bethe ansatz, observables are smooth functions of the integrals of motion. This allows for the construction of individual energy eigenstates that reproduce thermal predictions[27].

In Fig. 3a–c we demonstrate that the ETH is in fact the mechanism responsible for thermal behaviour in our non-integrable system. Figure 3c additionally shows that the second scenario mentioned above does not occur, because the fluctuations in the EONs $|C_\alpha|^2$ are large. Thermal behaviour also requires that both the diagonal and the chosen thermal ensemble have sufficiently narrow energy distributions $\rho(E)$ (the product of the probability distribution and the density of states), meaning that in the energy region where the energy distributions $\rho(E)$ are appreciable, the slope of the curve of the

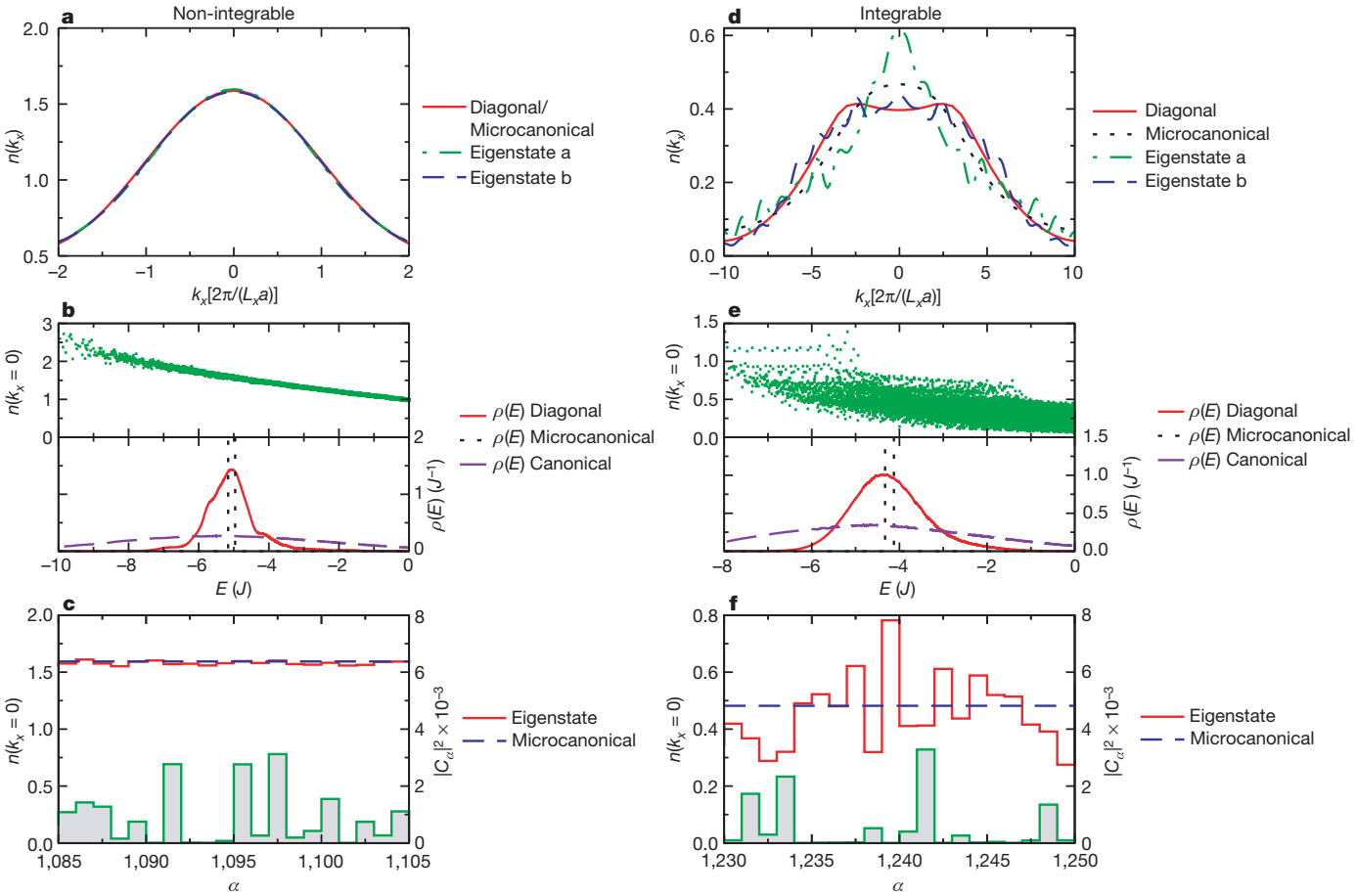

Figure 3 | Eigenstate thermalization hypothesis. **a**, In our non-integrable system, the momentum distribution $n(k_x)$ for two typical eigenstates with energies close to E_0 is identical to the microcanonical result, in accordance with the ETH. **b**, Upper panel: the EEV $n(k_x = 0)$, considered as a function of the eigenstate energy resembles a smooth curve. Lower panel: the energy distributions $\rho(E)$ (in units of J^{-1}) of the three ensembles we consider here. **c**, Detailed view of $n(k_x = 0)$ (left-hand scale) and $|C_\alpha|^2$ (right-hand scale) for 20 eigenstates around E_0. **d**, In the integrable system, the values of $n(k_x)$ for two eigenstates, a and b, with energies close to E_0 and for the microcanonical and diagonal ensembles are very different from each other; that is, the ETH fails. **e**, Upper panel: the EEV $n(k_x = 0)$, considered as a function of the eigenstate energy gives a thick cloud of points rather than resembling a smooth curve. Lower panel: the energy distributions in the integrable system are similar to the non-integrable ones depicted in **b**. **f**, Correlation between $n(k_x = 0)$ and $|C_\alpha|^2$ for 20 eigenstates around E_0. This correlation explains why in **d** the microcanonical prediction for $n(k_x = 0)$ is larger than the diagonal one.

EEV $A_{\alpha\alpha}$ plotted against energy (here $n(k_x=0)$ plotted against energy) does not change much; see Supplementary Discussion. As shown in Fig. 3b, this holds for the microcanonical and diagonal ensembles but not for the canonical ensemble, explaining the failure of the canonical ensemble to describe the relaxation in Fig. 1. We note that the fluctuations of the EONs $|C_\alpha|^2$ in Fig. 3b are artificially lowered by the averaging involved in the computation of the density of states (compare with Fig. 3c).

To strengthen the case for the ETH, we tested another observable. We chose it with the following consideration in mind: in our system interactions are local in space, and momentum distribution is a global, approximately spatially additive property. Thus, for the momentum distribution the ETH might arise through some simple spatial averaging mechanism. However, the ETH in fact does not depend on spatial averaging: for our final test of the ETH we chose an observable that is manifestly local in space, namely the expectation value of the occupation number of the central site of the lattice. We again found that the ETH holds (to within 3% relative standard deviation of eigenstate-to-eigenstate fluctuations).

On the other hand, Fig. 3d–f shows how the ETH fails for an isolated one-dimensional integrable system. The system consists of five hard-core bosons initially prepared in their ground state in an eight-site chain. We then link one of the ends of this chain to one of the ends of an adjoining (empty) 13-site chain to trigger relaxation dynamics. As Fig. 3e shows, $n(k_x)$ as a function of energy is a broad cloud of points, meaning that the ETH is not valid; Fig. 3f shows that the second scenario mentioned above does not occur in this system either.

Nevertheless, it might be possible for the first scenario to occur in this case, if the averages over the diagonal and the microcanonical energy distributions shown in Fig. 3e were to agree. Figure 3d shows that this does not happen. This is because, as shown in Fig. 3f, the values of $n(k_x=0)$ for the most-occupied states in the diagonal ensemble (the largest values of the EONs $|C_\alpha|^2$) are always smaller than the microcanonical prediction, and those for the least-occupied states are always larger. Hence, the usual thermal predictions fail because the correlations between the values of $n(k_x=0)$ and $|C_\alpha|^2$ preclude unbiased sampling of the former by the latter. These correlations have their origin in the non-trivial integrals of motion that make the system integrable and that enter the generalized Gibbs ensemble, which was introduced in ref. 3 as being appropriate for formulating the statistical mechanics of isolated integrable systems. In the non-integrable case shown in Fig. 3c, $n(k_x=0)$ is so narrowly distributed that it does not matter whether or not it is correlated with $|C_\alpha|^2$ (we have in fact seen no correlations in the non-integrable case). Again, we note that the fluctuations of the EONs $|C_\alpha|^2$ in Fig. 3e are artificially lowered, relative to those shown in Fig. 3f, by the averaging involved in the computation of the density of states.

The thermalization mechanism outlined thus far explains why long-time averages converge to their thermal predictions. A striking aspect of Fig. 1b, however, is that the time fluctuations are so small that after relaxation the thermal prediction works well at every instant of time. From equation (1), this might be suspected because the contribution of the off-diagonal terms is attenuated by temporal dephasing, which results from the generic incommensurability of the frequencies of the oscillating exponentials. However, this attenuation scales only as the square root of the number of dephasing terms, and is exactly compensated for by their larger number: if the number of eigenstates that have a significant overlap with the initial state is N_{states}, then the scaling of a typical C_α with N_{states} is $|C_\alpha| \sim 1/\sqrt{N_{\text{states}}}$, and the sum over off-diagonal terms in equation (1) finally does not scale down with N_{states}

$$\sum_{\substack{\alpha,\ \beta \\ \alpha\neq\beta}} \frac{e^{i(E_\alpha - E_\beta)t}}{N_{\text{states}}} A_{\alpha\beta} \sim \frac{\sqrt{N^2_{\text{states}}}}{N_{\text{states}}} A^{\text{typical}}_{\alpha\beta,\ \alpha\neq\beta} \sim A^{\text{typical}}_{\alpha\beta,\ \alpha\neq\beta}$$

where $A^{\text{typical}}_{\alpha\beta,\ \alpha\neq\beta}$ is the magnitude of a typical off-diagonal matrix element of the operator $\hat{A}$ between energy eigenstates that have significant overlaps with the initial state. Hence, if the magnitudes of the diagonal and off-diagonal terms were comparable, their contributions would also be comparable, and time fluctuations of the average would be of the order of the average. However, this is not the case, and thus

$$A^{\text{typical}}_{\alpha\beta,\ \alpha\neq\beta} \ll A^{\text{typical}}_{\alpha\alpha}$$

where $A^{\text{typical}}_{\alpha\alpha}$ is the magnitude of a typical diagonal matrix element of the operator $\hat{A}$ for an energy eigenstate that has a significant overlap with the initial state.

Figure 4a confirms this inequality for the matrix elements of the momentum distribution in our system. There is an a priori argument—admittedly dependent in part on certain hypotheses about chaos in quantum billiards—in support of this inequality in the case when the mean value of $\hat{A}$ in an energy eigenstate is comparable to the quantum fluctuation of $\hat{A}$ in that state[28].

On the other hand, the thermalization we see appears to be working a little too well: in a system as small as ours, we would expect measurement-to-measurement fluctuations to be much larger than is indicated in Fig. 1b. Indeed, as we show in Fig. 4b, the fluctuations that would actually be measured would be dominated by the quantum fluctuations of the time-dependent state. The rather large size of the quantum fluctuations relative to the thermal mean value is of course characteristic of small systems; however, the dominance of the quantum fluctuations over the temporal fluctuations of quantum expectation values is not, and is actually expected for generic systems in the thermodynamic limit[29].

We have demonstrated that, in contrast to the integrable case, the non-equilibrium dynamics of a generic isolated quantum system does lead to standard thermalization. We verified that this happens

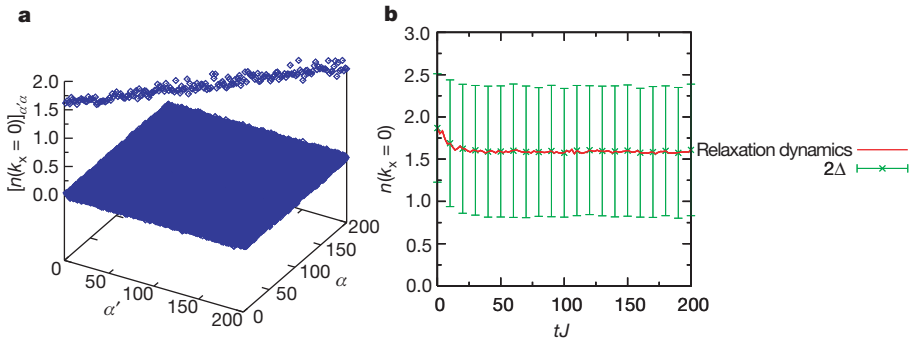

Figure 4 | Temporal versus quantum fluctuations. a, Matrix elements of the observable of interest $n(k_x=0)$ as a function of state indices; the eigenstates of the hamiltonian are indexed in the order of diminishing overlap with the initial state. The dominance of the diagonal matrix elements is apparent. **b**, The same time evolution as in Fig. 1b, with the error bars showing the quantum fluctuations $n(k_x=0) \pm \Delta$, where $\Delta = \left[\langle \hat{n}^2(k_x=0)\rangle - \langle \hat{n}(k_x=0)\rangle^2\right]^{1/2}$, which are clearly much larger than the temporal fluctuations of $n(k_x=0)$.

through the eigenstate thermalization mechanism, a scenario previously demonstrated[12] for the case of an integrable quantum hamiltonian weakly perturbed by a single matrix taken from a random gaussian ensemble, compellingly defended[13] for the case of rarefied semiclassical quantum billiards, and conjectured by both authors to be valid in general. Our results, when combined with the others we mentioned[12,13,20–27], constitute strong evidence that eigenstate thermalization indeed generally underlies thermal relaxation in isolated quantum systems. Therefore, to understand the existence of universal thermal time-asymptotic states, operator expectation values in individual eigenstates should be studied. This is a problem that is linear, time independent, and conceptually far simpler than any arising in current research on nonlinear dynamics of semiclassical systems. Among the fundamental open problems of statistical mechanics that could benefit from the linear time-independent perspective are the nature of irreversibility, the existence of a Kolmogorov-Arnold-Moser-like threshold[30] in quantum systems and the role of conserved quantities in the approach to equilibrium. Finally, having a clear conceptual picture for the origins of thermalization may make it possible to engineer new, 'unthermalizable' states of matter[12], with further applications in quantum information and precision measurement.

Received 7 December 2007; accepted 13 February 2008.

1. Kinoshita, T., Wenger, T. & Weiss, D. S. A quantum Newton's cradle. *Nature* **440,** 900–903 (2006).
2. Hofferberth, S., Lesanovsky, I., Fischer, B., Schumm, T. & Schmiedmayer, J. Non-equilibrium coherence dynamics in one-dimensional Bose gases. *Nature* **449,** 324–327 (2007).
3. Rigol, M., Dunjko, V., Yurovsky, V. & Olshanii, M. Relaxation in a completely integrable many-body quantum system: An ab initio study of the dynamics of the highly excited states of 1d lattice hard-core bosons. *Phys. Rev. Lett.* **98,** 050405 (2007).
4. Kollath, C., Läuchli, A. & Altman, E. Quench dynamics and nonequilibrium phase diagram of the Bose-Hubbard model. *Phys. Rev. Lett.* **98,** 180601 (2007).
5. Manmana, S. R., Wessel, S., Noack, R. M. & Muramatsu, A. Strongly correlated fermions after a quantum quench. *Phys. Rev. Lett.* **98,** 210405 (2007).
6. Burkov, A. A., Lukin, M. D. & Demler, E. Decoherence dynamics in low-dimensional cold atom interferometers. *Phys. Rev. Lett.* **98,** 200404 (2007).
7. Calabrese, P. & Cardy, J. Quantum quenches in extended systems. *J. Stat. Mech.* P06008 (2007).
8. Sengupta, K., Powell, S. & Sachdev, S. Quench dynamics across quantum critical points. *Phys. Rev. A* **69,** 053616 (2004).
9. Berges, J., Borsányi, S. & Wetterich, C. Prethermalization. *Phys. Rev. Lett.* **93,** 142002 (2004).
10. Gallavotti, G. *Statistical Mechanics: A Short Treatise* (Springer, Berlin, 1999).
11. Krylov, N. S. *Works on the Foundation of Statistical Physics* (Princeton Univ. Press, Princeton, 1979).
12. Deutsch, J. M. Quantum statistical mechanics in a closed system. *Phys. Rev. A* **43,** 2046–2049 (1991).
13. Srednicki, M. Chaos and quantum thermalization. *Phys. Rev. E* **50,** 888–901 (1994).
14. Sutherland, B. *Beautiful Models* 27–30 (World Scientific, Singapore, 2004).
15. Rigol, M., Muramatsu, A. & Olshanii, M. Hard-core bosons on optical superlattices: Dynamics and relaxation in the superfluid and insulating regimes. *Phys. Rev. A* **74,** 053616 (2006).
16. Cazalilla, M. A. Effect of suddenly turning on interactions in the Luttinger model. *Phys. Rev. Lett.* **97,** 156403 (2006).
17. Jin, D. S., Ensher, J. R., Matthews, M. R., Wieman, C. E. & Cornell, E. A. Collective excitations of a Bose-Einstein condensate in a dilute gas. *Phys. Rev. Lett.* **77,** 420–423 (1996).
18. Greiner, M., Mandel, O., Esslinger, T., Hänsch, T. W. & Bloch, I. Quantum phase transition from a superfluid to a Mott insulator in a gas of ultracold atoms. *Nature* **415,** 39–44 (2002).
19. Mandel, O. *et al.* Controlled collisions for multi-particle entanglement of optically trapped atoms. *Nature* **425,** 937–940 (2003).
20. Horoi, M., Zelevinsky, V. & Brown, B. A. Chaos vs thermalization in the nuclear shell model. *Phys. Rev. Lett.* **74,** 5194–5197 (1995).
21. Shnirelman, A. I. Ergodic properties of eigenfunctions. *Usp. Mat. Nauk* **29,** 181–182 (1974).
22. Voros, A. *Stochastic Behavior in Classical and Quantum Hamiltonian Systems* (Springer, Berlin, 1979).
23. de Verdière, Y. C. Ergodicité et fonctions propres du Laplacien. *Commun. Math. Phys.* **102,** 497–502 (1985).
24. Zelditch, S. Uniform distribution of eigenfunctions on compact hyperbolic surfaces. *Duke Math. J.* **55,** 919–941 (1987).
25. Heller, E. J. & Landry, B. R. Statistical properties of many particle eigenfunctions. *J. Phys. A* **40,** 9259–9274 (2007).
26. Berry, M. V. Regular and irregular semiclassical wavefunctions. *J. Phys. A* **10,** 2083–2091 (1977).
27. Korepin, V. E., Bogoliubov, N. M. & Izergin, A. G. *Quantum Inverse Scattering Method and Correlation Functions* 40–41 (Cambridge Univ. Press, Cambridge, 1993).
28. Srednicki, M. Does quantum chaos explain quantum statistical mechanics? Preprint at ⟨http://arXiv.org/abs/cond-mat/9410046⟩ (1994).
29. Srednicki, M. Thermal fluctuations in quantized chaotic systems. *J. Phys. A* **29,** L75–L79 (1996).
30. José, J. V. & Saletan, E. J. *Classical Dynamics: A Contemporary Approach* 474–491 (Cambridge Univ. Press, Cambridge, 1998).

Supplementary Information is linked to the online version of the paper at www.nature.com/nature.

Acknowledgements We thank A. C. Cassidy, K. Jacobs, A. P. Young, and E. J. Heller for their comments. We acknowledge financial support from the National Science Foundation and the Office of Naval Research. We are grateful to the USC HPCC centre, where all our numerical computations were performed.

Author Information Reprints and permissions information is available at www.nature.com/reprints. Correspondence and requests for materials should be addressed to M.O. (maxim.olchanyi@umb.edu).

CORRECTIONS & AMENDMENTS

ERRATUM

doi:10.1038/nature10773

Thermalization and its mechanism for generic isolated quantum systems

Marcos Rigol, Vanja Dunjko & Maxim Olshanii

Nature **452,** 854–858 (2008).

In Figs 3b and e of this Letter, there were two points that could have been misinterpreted as outlying data points (they were inadvertently printed parts of a key to the figure that was incompletely removed). These points have been removed in the HTML and PDF versions. We thank David S. Weiss for drawing this to our attention.